SUPPORTING INFORMATION

Failure Mechanisms at Interfaces between Lithium Metal Electrodes and a Single-ion Conducting Polymer Gel Electrolyte

Louise Frenck[a,b,†], Peter Lennartz[c,d,†], Dilworth Y. Parkinson[e], Martin Winter[c,f], Nitash P. Balsara[a,b], Gunther Brunklaus[c*]*

[a]Department of Chemical and Biomolecular Engineering, University of California, Berkeley, California 94720, United States

[b]Materials Sciences Division, Lawrence Berkeley National Laboratory, Berkeley, California 94720, United States

[c]Forschungszentrum Jülich GmbH, Helmholtz-Institute Münster (IEK-12), Corrensstr. 46, 48149 Münster, Germany

[d]University of Duisburg-Essen, Faculty of Physics, Lotharstr. 1-21, 47048 Duisburg, Germany

[e]Advanced Light Source, Lawrence Berkeley National Laboratory, Berkeley, California 94720, United States

[f]University of Münster, MEET Battery Research Center, Institute of Physical Chemistry, Corrensstr. 46, 48149 Münster, Germany

[†]Contributed equally to this work

*Corresponding authors: g.brunklaus@fz-juelich.de; nbalsara@berkeley.edu

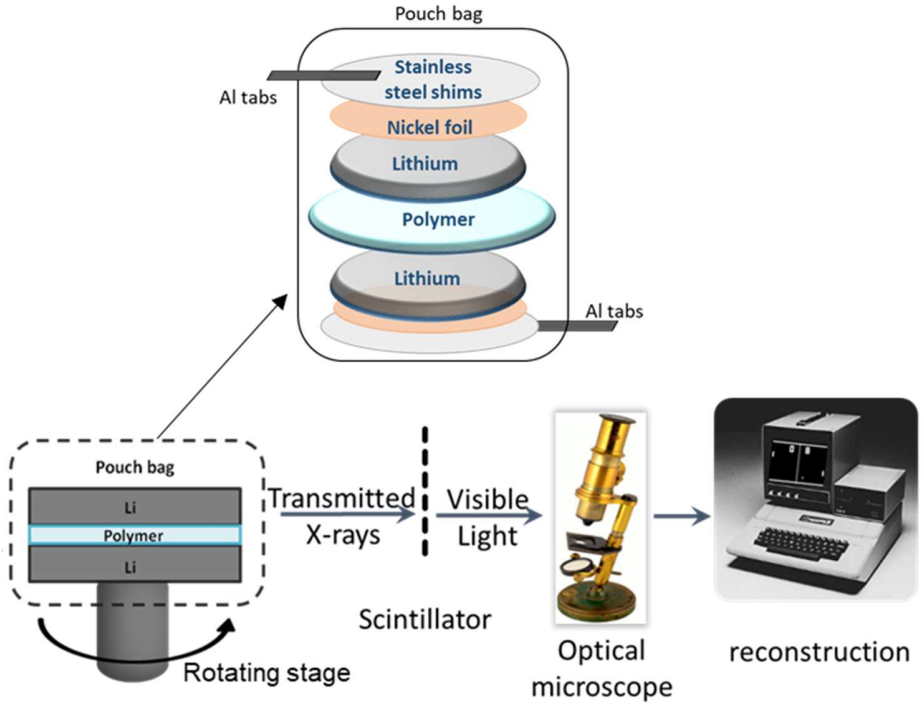

Figure S1: *Schematic of the cell set-up containing two symmetric Li electrodes and the polymer membrane inside a sealed pouch bag. The lithium foil is pressed onto Nickel current collectors and stainless-steel shims are added for horizontal alignment during tomography. The cell is rotated for complete spatial resolution. X-ray tomography images are reconstructed by a combination of a scintillator, optical microscope and software.*

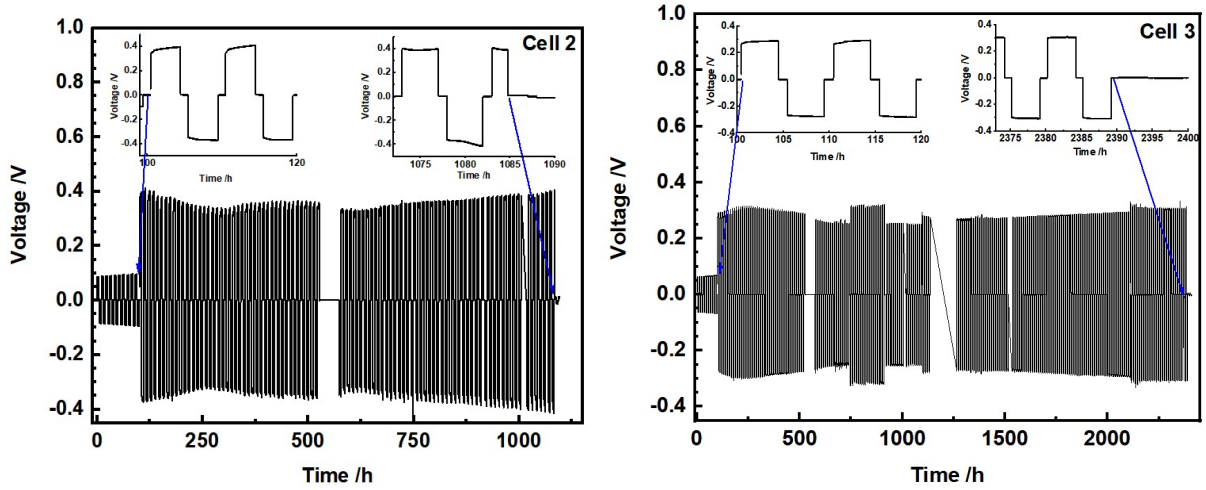

Figure S2: *Overvoltage profiles of two Li||Li cells cycling at 25 °C and a current density of 0.1 mA cm^{-2} (capacity of 0.4 mAh cm^{-2}). Each full cycle takes approximately 10 h, including 8 h of stripping and plating and rest steps for impedance measurements. Conditioning cycles were performed at 0.02 mA/cm² for the first 100 h. Cell 2 performs substantially shorter than Cell 3, as discussed in the main document.*

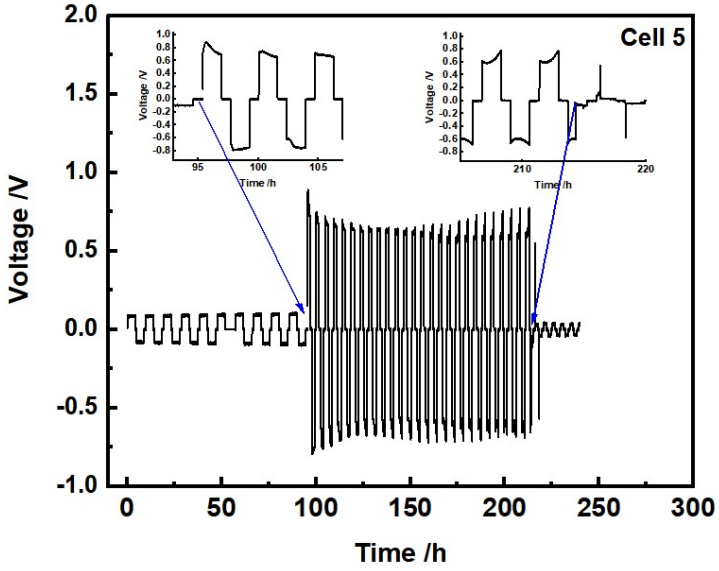

Figure S3*: Overvoltage profile of a Li||Li cell cycling at 25 °C and a current density of 0.3 mA cm^{-2} (capacity of 1.2 mAh cm^{-2}). Each full cycle takes approximately 10 h, including 8 h of stripping and plating and rest steps for impedance measurements. Conditioning cycles were performed at 0.02 mA/cm² for the first 100 h.*

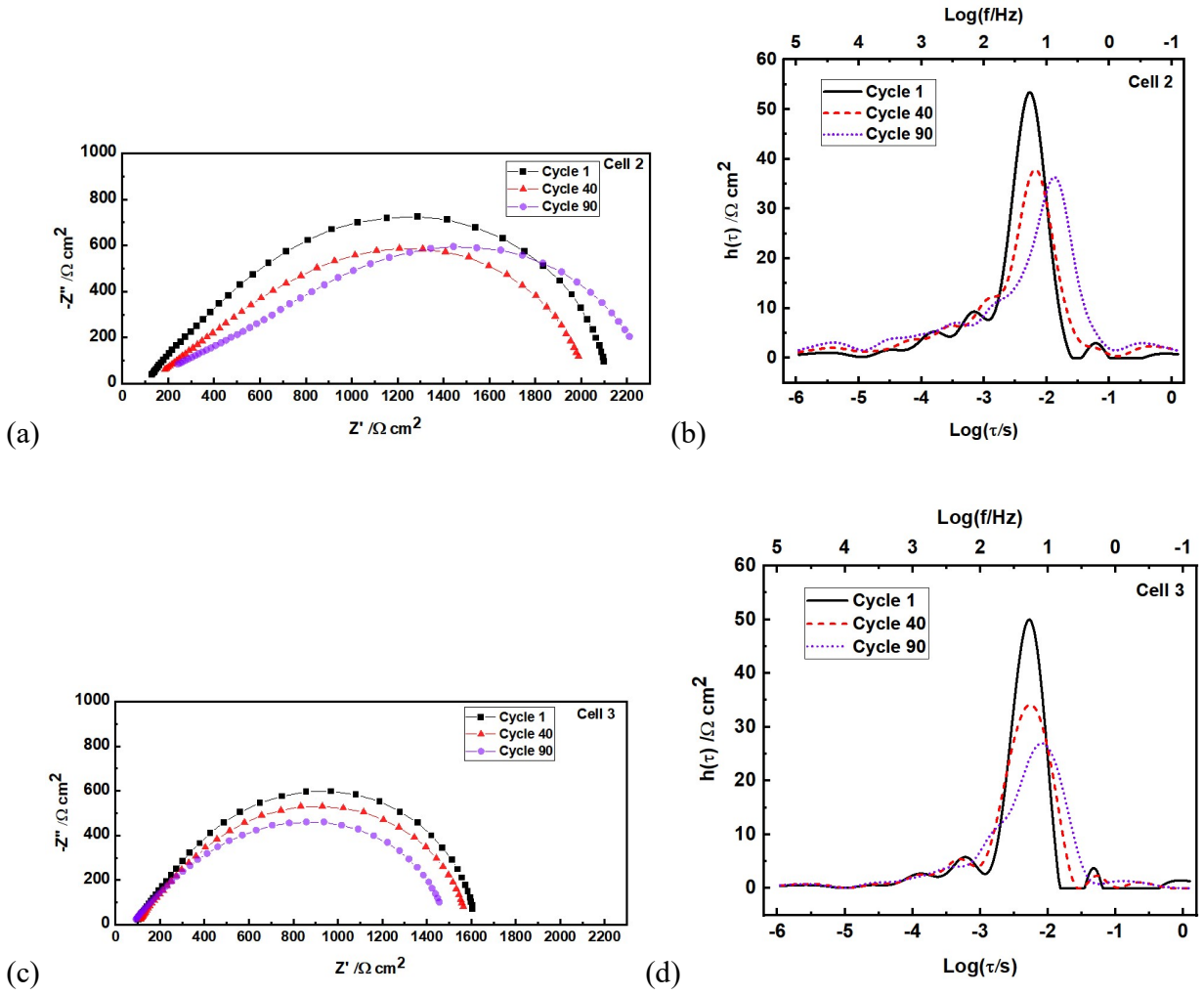

Figure S4: *(a)(c): Nyquist plots and DRT plots of Cell 2 and 3 after one, 40 and 90 cycles at a current density of i = 0.1 mA cm^{-2}. Impedance spectra were measured after 45 min of equilibration at OCV after each cycle. (b)(d): DRT analysis of the different cells at cycle one, 40 and 90. The development of interfacial resistance and time constants for Cell 3 is comparable to that of Cell 1 in the main document.*

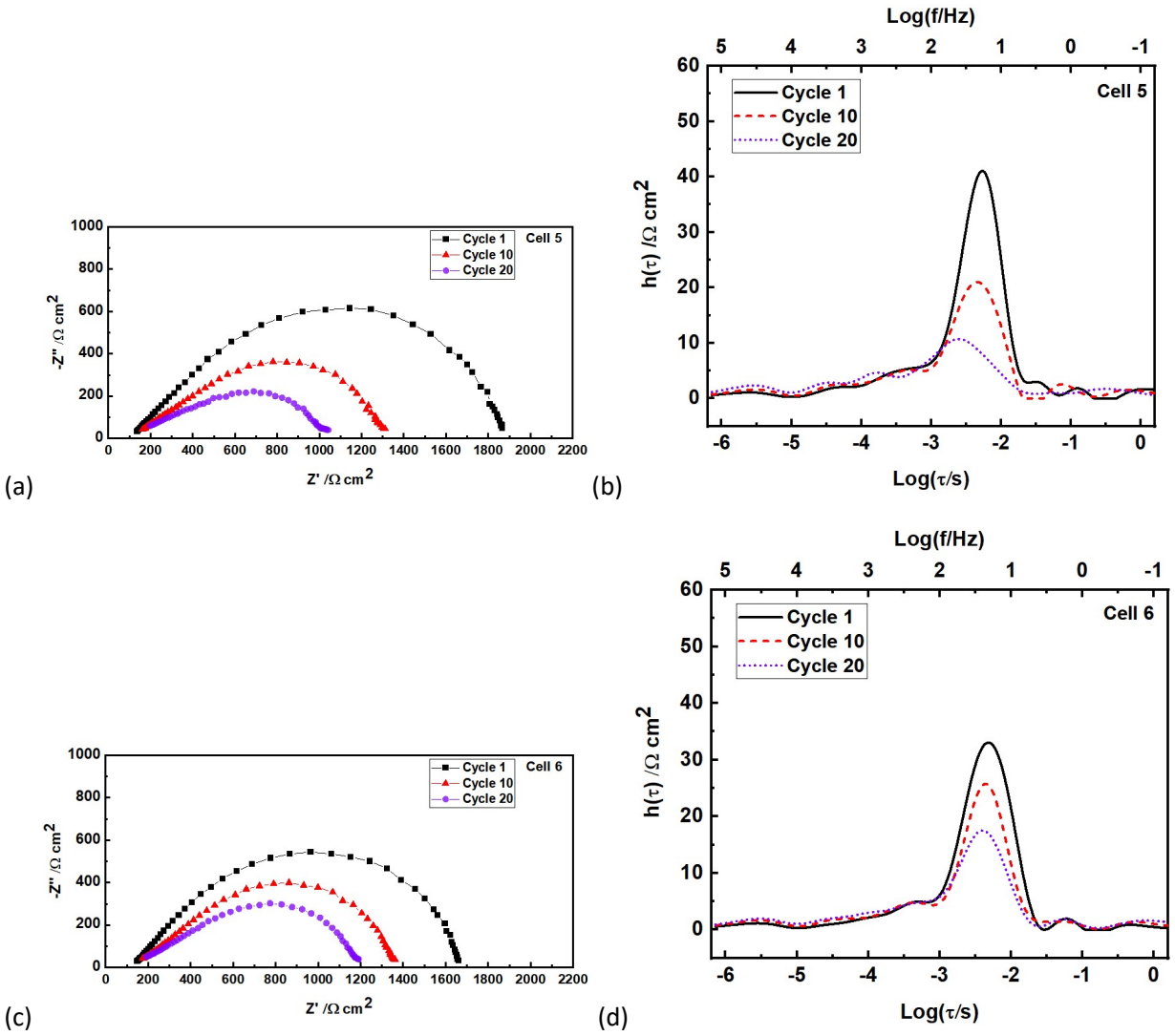

Figure S5: *(a)(c) Nyquist plots and DRT plots of Cell 5 and 6 after one, 10 and 20 cycles at a current density of i = 0.3 mA cm^{-2}. Impedance spectra were measured after 45 min of equilibration at OCV after each cycle. (b)(d): DRT analysis of Cell 5 and 6 after one, 10 and 20 cycles. The development of interfacial resistance and time constants for Cell 5 and 6 is comparable to that of Cell 4 in the main document.*

Details of the DRT analysis:

The DRT algorithm is based on Danzer [1], with the adaption that purely capacitive and inductive elements are neglected due to the smaller frequency window and no visible capacitive or inductive

characteristics in the spectra. Thus, the equivalent circuit is based on an Ohmic resistor in series with many RC-elements, which can be characterized by a resistance h_k and capacitance C_k or by the time constant $\tau_k = h_k C_k$.

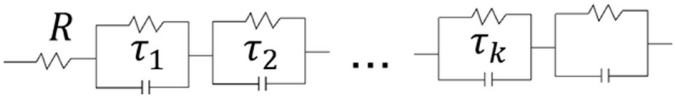

The associated equation for impedance response $Z(\omega)$ of this equivalent circuit is given in **Equation S1**:

$$Z(\omega) = R + \sum_k \frac{h_k}{1 + j\omega\tau_k} \qquad \textbf{(Equation S1)}$$

With Ohmic resistance $[\Omega\mathrm{cm}^2]$, resistive capacitive contribution $h_k[\Omega\mathrm{cm}^2]$, imaginary number j and angular frequency $\omega = 2\pi f$. Next, the time constants are distributed over a large range (inverse frequency window) to cover all responses present in the measured spectrum. The equivalent circuit is fitted to the actual spectrum with a non-negative least squares minimization and the additional constraint of Tikhonov regularization [2], which regulates unphysical oscillation (mathematically correct solutions which are not meaningful in the physical application of a continuous capacitive interface). A schematic overview of the algorithm is shown in **Figure S6**:

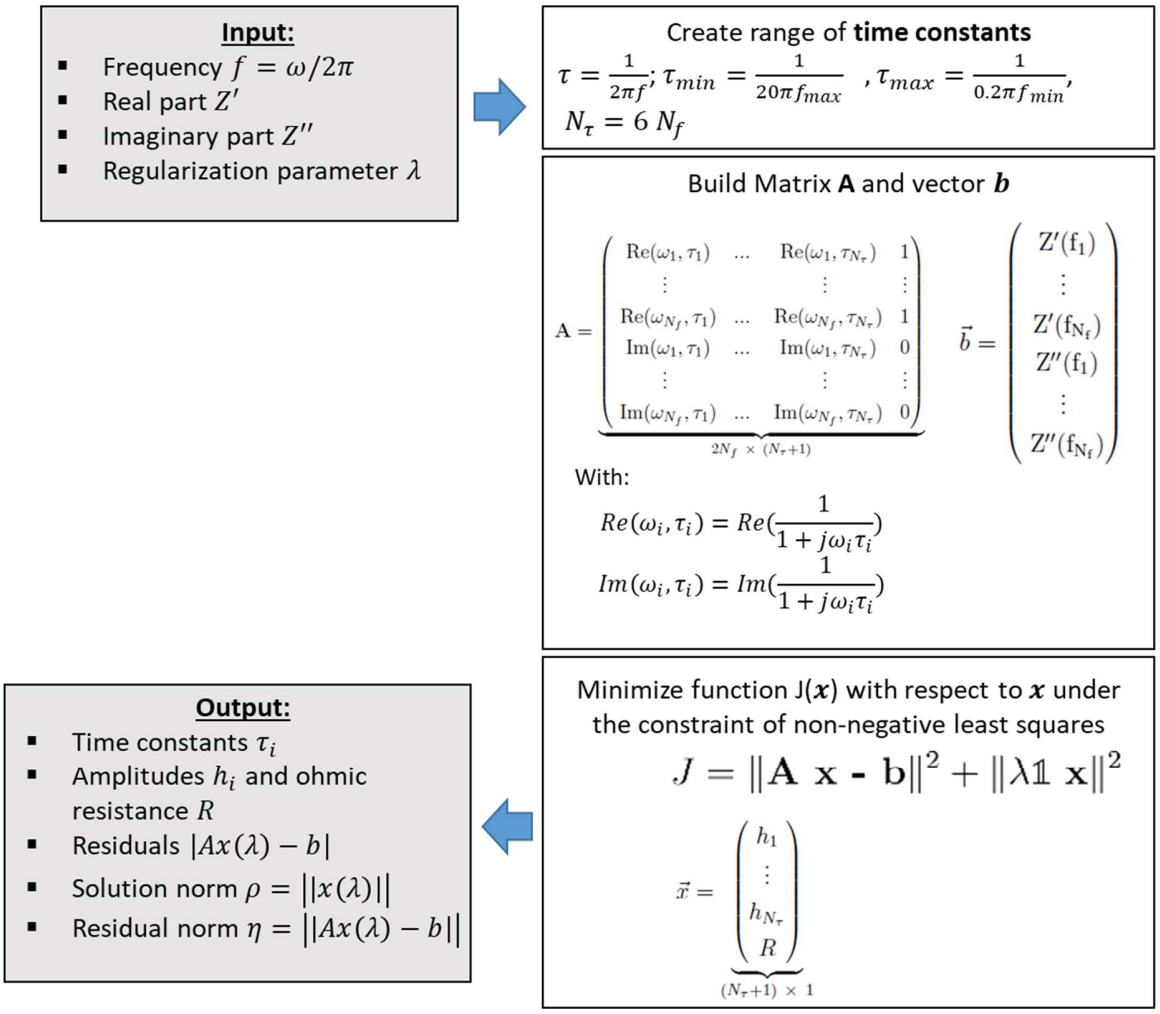

Figure S6*: Scheme of the DRT algorithm which calculates the Ohmic resistance, as well as the resistive-capacitive contribution of each RC-element.*

The regularization parameter λ influences the sharpness of the peaks: Too large values cause over-smoothening of the spectrum, whereas too small values may result in artificial peaks which are unphysical. A value of $\lambda = 0.1$ was chosen as a compromise between low residual norm and low solution norm. **Figure S7** demonstrates that at a value of $\lambda = 0.1$, the residual norm is still relatively small. Lower values of λ would decrease the residual norm even further, but lead to an increase in the solution norm.

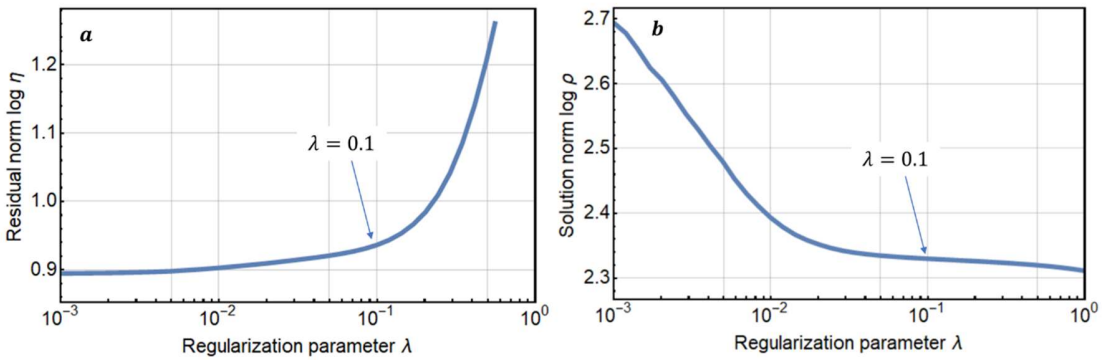

Figure S7*: Logarithm of (a) the residual norm and (b) the solution norm of Cell 1 before cycling as example to demonstrate that at a value of* $\lambda = 0.1$*, the residual norm is still relatively small. Lower values of* λ *would decrease the residual norm (a) even further but lead to an increase in the solution norm (b).*

Since the DRT algorithm is sensitive towards noise, a reduced frequency window is considered for evaluation and shown in **Figure S8**.

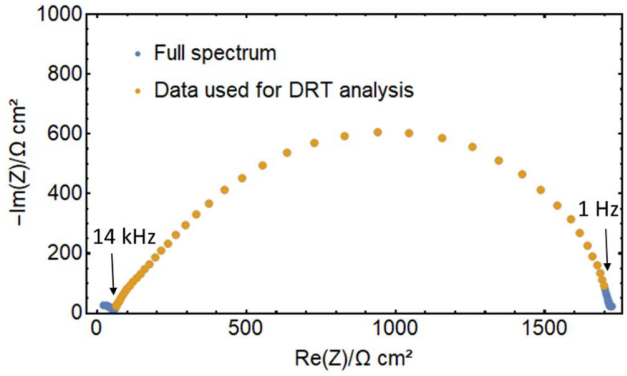

Figure S8: *Exemplary spectrum of Cell 1 before cycling at 25 °C to demonstrate the range of data points taken into consideration for DRT analysis. The high-frequency semi-circle contribution is associated with bulk electrolyte resistance (geometric capacitance) and typically occurs in polymer electrolyte systems, as the ionic conductivity is low enough to shift this contribution to the observed frequency domain [3].*

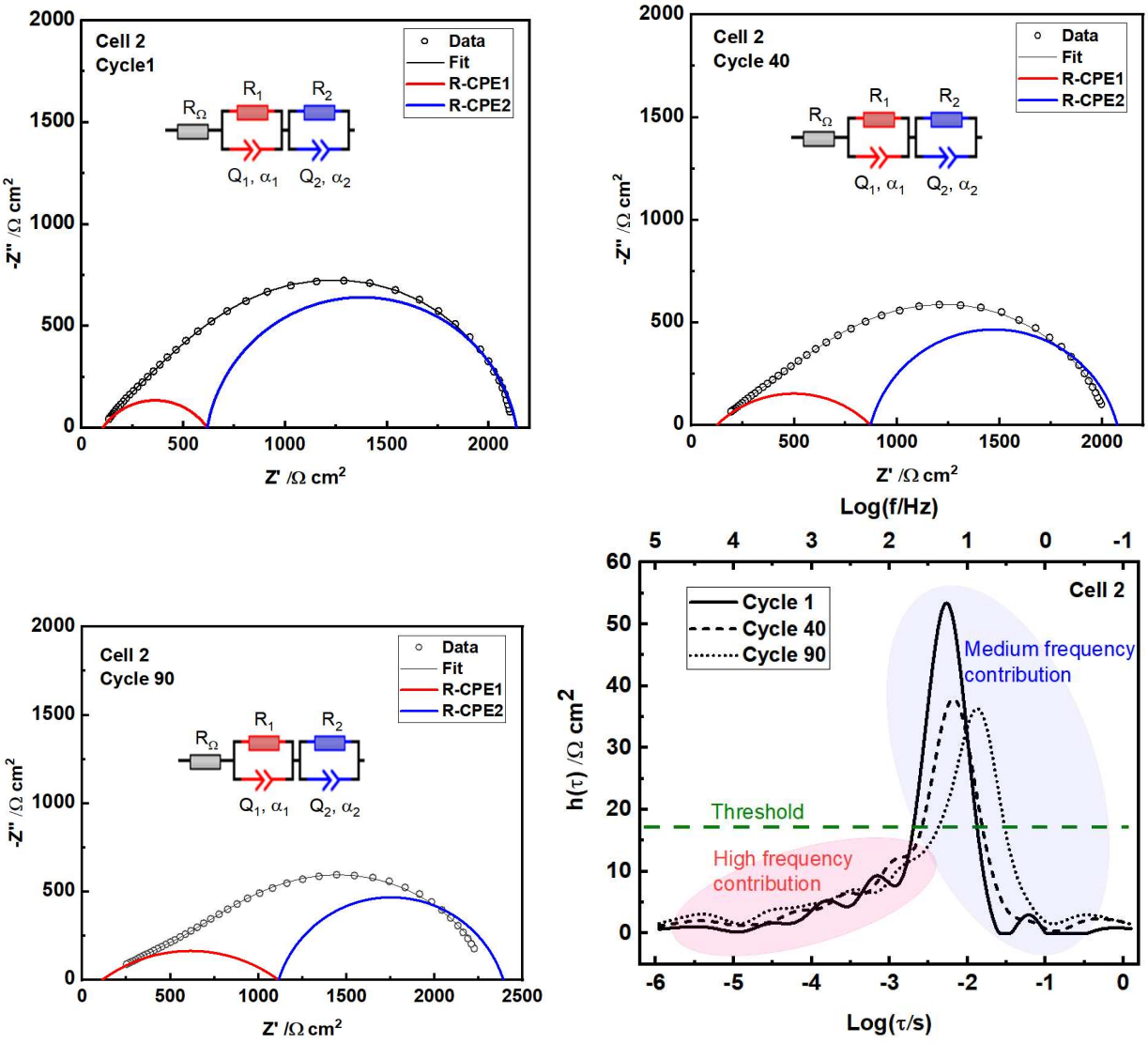

Figure S9: *Equivalent circuit modeling of Cell 2 as representative example. The equivalent circuit consists of a resistor in series (modeling bulk resistance) and two R-CPE elements, modeling imperfect interfaces. The DRT spectrum reveals one authentic peak in the medium frequency range, which can be modelled with an R-CPE element. At higher frequencies, the peaks are not clearly separable and do not correspond to a single R-CPE element. Modeling of the high-frequency region with a simple equivalent circuit model fails, as the response is too broad in frequency range and the α value of the CPE becomes unrealistically low (<0.7), especially after prolonged cycling. Instead of detailed equivalent circuit modeling, each DRT spectrum in this work is directly used for calculation of the interfacial resistance by numerical integration of the whole spectrum (the area corresponds to the summed interfacial resistance).*

Table ST1: *Fit parameters of the invoked equivalent circuit model.*

Equivalent circuit fit Cell 2	Cycle 1	Cycle 40	Cycle 90
Ohmic Resistance R_Ω /$\Omega\mathrm{cm}^2$	103.6	123.1	112.8
Resistance $R_1/\Omega\mathrm{cm}^2$	513.5	749.4	1002.0
Pseudo capacitance Q_1	5.2E-06	1.0E-05	1.4E-05
CPE factor α_1	0.62	0.49	0.40
Resistance R_2 /$\Omega\mathrm{cm}^2$	1519.3	1201.3	1276.1
Pseudo capacitance Q_2	1.5E-06	2.8-06	5.1E-06
CPE factor α_2	0.89	0.84	0.81

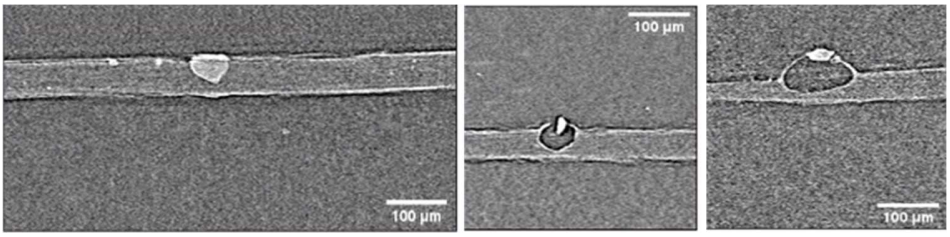

Figure S10: *Cross-sectional slices through the reconstructed X-ray tomograms representing different electrolyte impurity sizes and morphology.*

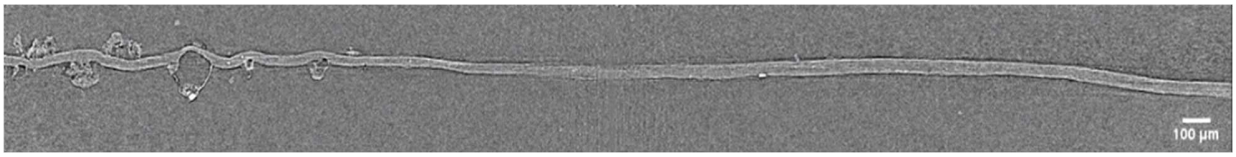

Figure S11*. Cross section tomogram of a failed cycled symmetric Li||Li cell showing non-planar and planar Li electrodeposition. Non-planar deposits are localized in a small region toward the left side of the tomogram. Planar Li-electrodeposition is seen over a large area of the cell in spite of the presence of a few impurities (bright spots) that could have nucleated non-planar structures.*

REFERENCES

[1] Danzer, M. A. Generalized Distribution of Relaxation Times Analysis for the Characterization of Impedance Spectra, Batteries 2019, 5 (3), 53

[2] Weese, J. A reliable and fast method for the solution of Fredhol integral equations of the first kind based on Tikhonov regularization, Computer Physics Communications 1992, 69 (1), 99

[3] Brandell, D.; Mindemark, J.; Hernández, G. *Polymer-based Solid State Batteries*; De Gruyter, 2021.